

Sławomir KOWALSKI\*

## ANALYSIS OF THE POSSIBILITIES OF USING CrN+a-C:H:W COATINGS TO MITIGATE FRETTING WEAR IN PUSH FIT JOINTS OPERATING IN ROTATIONAL BENDING CONDITIONS

### ANALIZA MOŻLIWOŚCI ZASTOSOWANIA WYBRANYCH POWŁOK DIAMOND-LIKE-CARBON CELEM OGRANICZENIA ZUŻYCIA FRETTINGOWEGO W POŁĄCZENIACH WCISKOWYCH PRACUJĄCYCH W WARUNKACH ZGINANIA OBROTOWEGO

**Key words:**

fretting wear, wheel set, PVD coating, rotational bending, CrN+a-C:H:W.

**Abstract**

In this article, the results of wear tests of a push fit joint operating in rotational bending conditions have been presented. The assumed operation conditions were similar to those for a real rail vehicle wheel set. Samples made of uncoated C45 steel and those in which shafts were covered with a CrN+a-C:H:W coating were analysed. The push fit joint was loaded with 550 N, and it completed  $8 \times 10^6$  cycles. Following wear tests, the macroscopic and microscopic observations of the shaft top layer were conducted to determine the intensity of fretting wear development. The former demonstrated that, in the case of uncoated shafts, wear occurs on either side of the joint, in the form of a maximum 2 mm wide ring. The use of protective coatings significantly reduced damage to the shaft top layer. Traces of fretting wear occur occasionally at the shaft circumference and affect small areas. The microscopic observations and EDS analysis of the chemical composition of the areas affected by fretting demonstrated mainly wear in the form of the build-up of material originating from, first of all, the shearing of sleeve top layer micro-irregularities that underwent plastic deformation and then oxidation.

**Słowa kluczowe:**

zużycie frettingowe, zestaw kół, powłoka PVD, zginanie obrotowe, CrN+a-C:H:W.

**Streszczenie**

W artykule zaprezentowano wyniki badań zużyciowych połączenia wciskowego pracującego w warunkach zginania obrotowego. Przyjęte warunki pracy zbliżone były do warunków pracy rzeczywistego zestawu kołowego pojazdów szynowych. Analizie poddano próbki wykonane ze stali C45 bez powłoki oraz próbki, w których wały pokryto powłoką CrN+a-C:H:W. Połączenie wciskowe obciążone zostało siłą 550N i wykonało  $8 \times 10^6$  cykli. Po badaniach zużyciowych przeprowadzono obserwacje makroskopowe i mikroskopowe warstwy wierzchniej wałów w celu określenia intensywności rozwoju zużycia frettingowego. Te pierwsze wykazały, że w przypadku wałów bez powłoki zużycie występuje po obu stronach połączenia w postaci pierścienia o maksymalnej szerokości 2 mm. Zastosowanie powłok ochronnych zdecydowanie zmniejszyło uszkodzenia warstwy wierzchniej wałów. Ślady zużycia frettingowego występują sporadycznie na obwodzie wałka i zajmują niewielkie obszary. Obserwacje mikroskopowe oraz analiza EDS składu chemicznego obszarów zajętych przez zjawisko frettingu wykazały w głównej mierze zużycie w postaci nalepów materiału pochodzącego przede wszystkim ze ścinania mikronierówności warstwy wierzchniej tulei, które uległy deformacji plastycznej, a następnie utlenieniu.

## INTRODUCTION

Various methods of element joining are used in machinery construction. One of those methods is push fit joints, which are simple and can be made easily, and can transfer relatively high axial loads as well as

static and dynamic torques. Those features cause push fit joints to be used for connecting elements operating in particularly difficult conditions with variable loads. Cyclic rotational bending is an example of such operation conditions. Both bending and contact stresses occur there at the same time. Rail vehicle wheel sets

\* State Higher Vocational School in Nowy Sącz, 1a Zamenhofa street, 33-300 Nowy Sącz, Poland, e-mail: skowalski@pwsz-ns.edu.pl.

are an example of a push fit joint operating in rotational bending conditions. The set operates in particularly harsh conditions described further in this work, which make the joint more susceptible to damage and wear. Fretting wear, which may generate fatigue wear and, consequently, cause the joint to become loose or cracked, is an example of damage to forced-in joints.

As one of the most important elements, a wheel set should be distinguished by particularly high operational parameters. Hence, the test methodology in this article is based on the wheel set operation conditions. If test results are satisfactory, the proposed solutions regarding top layer finish with DLC coatings will be able to be compared with real wheel sets.

Attempts to improve the life of forced-in joints operating in rotational bending conditions by means of various methods are of interest to many scientists. New solutions, for example those regarding materials and additional axle top layer finish treatments such as nitriding, surface hardening, or rolling were compared. All those procedures failed to produce satisfactory results. That is why an attempt was made to use an innovative solution, that being a shaft covering with hard protective coatings. The review of literature available to the author indicates that such a solution has not been used yet.

At present, protective coatings are used not only as a protection for cutting tools, but also of elements operating in various conditions. Various coating alternatives are available on the market ranging from single to double and multi-layer coatings applied by means of the CVD and PVD methods. Innovative coatings are also made and subjected to wear tests so that even better solutions can be arrived at. Depending on the workmanship, coatings differ in thickness or in the coefficient of friction, but each of those coatings protects an element from damage to some extent. One of the coatings distinguished by high wear resistance is a diamond-like-carbon coating. Those coatings were discovered by Aisenberg and Chabot, who obtained hydrogen-free amorphous layers by chilling a low-energy carbon ion beam in argon. As it turned out, that discovery was a breakthrough [L. 1–2], because it became apparent that those coatings are distinguished by high hardness and a low coefficient of friction. They have various structures, and their properties depend on the way and parameters of fabrication. Other features that weigh in favour of an attempt to use those coatings in forced-in joints operating in rotational bending conditions are high wearing resistance and chemical stability. Those properties are confirmed in numerous publications. Works [L. 3–9] can be mentioned as demonstration articles in which the assessment of the properties of the coatings in various conditions was undertaken.

At present, DLC coatings are more and more often used for plating of, among other things, the elements of a combustion engine, computers, and orthopaedic implants, in particular, hip and knee joints [L. 10–12].

## ABOUT FRETTING WEAR

Fretting wear belongs to the group of tribological kinds of wear. In view of the complexity of physical and chemical phenomena accompanying wear and because of its mechanism depending on, among other things, the assumed test methodology and operation conditions, the unambiguous definition of wear has not been given to date. Based on the review of literature, it may be stated that fretting wear is a process of the destruction of the top layer of mating elements that occurs during the small mutual displacement of those surfaces caused by the vibrations of small amplitude.

The precise number of factors influencing the development of wear is unknown. In his work [L. 13], Bill R.C. mentions three groups of factors that are most often taken into account during tests and which may influence the development of wear.

In the first group, he included the conditions of the oscillation of tangential displacement such as a load on the sample, vibration amplitude and frequency, the number of cycles, and the geometry of the mating top layers. Many pieces of literature can be found in which authors take the influence of those factors on fretting wear development into consideration. For example, the influence of the slip amplitude and normal load on the development of wear in tubular elements made of 690 alloy were examined in [L. 14]. Work [L. 15] concerns the experimental testing of the influence of grit blasting of the top layer of the elements made of Al7075-T6 alloy with the value of cyclic normal loads taken into account. An innovative test bed and the finite element method were used for the tests. In work [L. 16], the development mechanism of fretting wear under the influence of complex cyclic loads was examined. Tests demonstrated, among other things, that the cyclic normal load enlarges the slip area of the elements' surfaces thus causing the displacement of crack nuclei towards the middle of the joint.

The second group of factors is related to the properties of materials used for the construction of the elements being tested. These include hardness, top layer geometry, adhesion properties, fatigue strength, tensile strength, and the yield point. Sample works in which the influence of those factors was examined include work [L. 17], in which the influence of top layer topography on the development of the flat-on-flat contact wear was examined. Work [L. 18] concerns the influence of various hardnesses of the mating elements on fretting wear development. Surfaces in the ball-on-flat contact were examined. Work [L. 19] concerned the testing of the influence of top layer hardness of the elements made of AISI steel.

The third group of factors are the environmental conditions, and Bill R.C. included temperature, humidity, pollutants, and lubrication in that group. The author of [L. 20] examined the impact of ambient temperature on fretting wear development. Tests were conducted for

various values of the displacement amplitude at ambient temperature and at a temperature in the order of 620°C. Work [L. 21] examined the influence of various relative humidity values on fretting wear of the ball-on-flat joint between a surface made of 7075 aluminium alloy and a ball made of 52100 bearing steel. The authors of work [L. 22] examined the influence of a lubricating medium on fretting wear of the surfaces of elements made of CuNiAl and 42CrMo4 in the flat-on-flat contact. The authors demonstrated that the wear mechanism depends on the lubricating medium. Oil and filtrated sea water were used as the lubricating medium.

The image of fretting wear may include traces of corrosion on the surface of the elements, the increase of top layer roughness, microcracks and micro pits, etc., and the consequences of those kinds of damage, in the case of push fit joints, include the reduction of surface pressures.

Fretting wear is found in many areas of technology. For example, fretting wear is observed in orthopaedic elements and those connecting broken bones [L. 23–25], in the structural elements of airplanes [L. 26–28], in the elements of nuclear power plants, and in the space industry [L. 29–31], in steel ropes used, among other areas, in mining industry and cableways [L. 32–34], in the elements of rail vehicles and infrastructure [L. 35–37], etc. Fretting wear also occurs in push fit joints. In view of technical problems connected with joint disassembly and then with wear observations, few authors discuss fretting wear in these joints. Sample works in that area include [L. 38–39]. That joint does, however, accumulate in it all the factors essential to the initiation and development of fretting wear. There is a specific pressure between the surfaces of the connected elements, and the relative displacement of those surfaces occurs [L. 39].

In his numerous works, Guzowski S. examined and also proposed the fretting wear development mechanism in a push fit joint loaded with a bending moment in rotational bending conditions. Tests were conducted for forced-in and thermo-compression joints with three factors taken into consideration including the way the joint was made, the tolerance value, and the roughness of the elements being connected.

Test results demonstrated that the mutual interaction of those factors is strongly interdependent on those factors. For example, the increase of the tolerance value reduces wear intensity in a thermo-compression bonding, and it significantly increases that intensity in a forced-in joint.

Based on the experiments, the author suggested the development mechanism for fretting wear in forced-in joints [L. 39] as follows:

- Creation, as a result of a push fit joint to have been made, of the areas of the actual contact of the surfaces being connected;
- The generation of oscillatory tangential displacement at the interface between the surfaces of the elements

as a result of joint loading with a bending moment in rotational bending conditions;

- The creation of adhesive bonds in the areas of the actual contact of the first bodies, which bonds are subsequently broken thus forming gaps and build-up at contact surfaces;
- The shearing and smudging of surface damage arisen as a result of adhesive bond breaking;
- The oxidation of the previously damaged area;
- The micromachining of the opposite surface with the asperities of oxidised build-up;
- The forming of wear products as a result of the micromachining and cracking of the thin oxide layer – the rise of the third body and wear process stabilisation; and,
- In the event that oscillation continues to occur, the removal of the third body from the contact area, but only close to joint edges, which leads to the repeated creation of adhesive bonds and their continuation.

It follows from the wear mechanism presented that fretting consists of the following kinds of wear: adhesive wear which destroys the mating surfaces in an intensive way thus creating deep cavities and material build-up, abrasive wear consisting in the destruction of the top layer by the formed and moving wear products, corrosive wear caused by the formation of oxides at the joint contact surface (the wear products, which became oxidised, are very hard, which may accelerate the wear process), and fatigue wear following from the permissible stresses at the contact surface being exceeded. The result of that will be the formation of microcracks and, consequently, the reduction of the fatigue strength of the material.

#### OPERATION CONDITIONS OF THE WHEEL SET AND TEST MODEL

While analysing fretting wear in forced-in joints, it was assumed that the operation conditions of the model being tested would be similar to those of the rail vehicle wheel set. This is one of the most important elements of a rail vehicle; therefore, a wheel set should be distinguished by its long life and high reliability. However, the loads during operation cause the reduction of wheel set reliability sooner than in the case of other subassemblies, which may, in turn, be the cause of premature damage to the wheel set. Uncontrolled wear and damage, particularly occurring unexpectedly and suddenly, may lead to train derailing thus causing serious consequences in the form of costly damage to railway infrastructure and, in extreme cases, to the death of many people. Events with hundreds of casualties have taken place many times in recent years. These statements provide even more motivation for seeking solutions that will improve the life of wheel sets. During operation, the forces presented in **Figure 1** act on the wheel set; however, the presented load distribution on the wheel set occurs in the case of a ride along a curve.

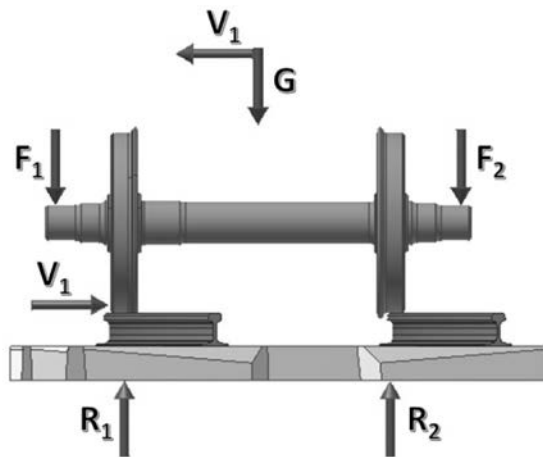


**Fig. 1. Load distribution on the wheel set during a ride along a curve, where:**

$G$  – the gravity force of the rail vehicle,  
 $V_1$  – lateral force acting on the edge of running wheels in the case of rides along a curve. The magnitude of that force depends on the wheel location in relation to the rail head,  
 $F_1, F_2$  – vertical concentrated forces acting on axle pins, originating from the vehicle weight,  
 $R_1, R_2$  – vertical force reactions at the interface between the wheel and the rail

**Rys. 1. Rozkład obciążenia zestawu kołowego podczas jazdy po łuku, gdzie:**

$G$  – siła ciężkości pojazdu szynowego,  
 $V_1$  – siła boczna działająca na obrzeże kół tocznych w przypadku jazdy po łuku. Wielkość jej zależy od położenia koła względem główki szyny,  
 $F_1, F_2$  – pionowe siły skupione działające na czopy osi, pochodzące od masy pojazdu,  
 $R_1, R_2$  – reakcje sił pionowych, występujące na styku koła z szyną

The result of the operation of the presented loads is the generation of a bending moment, whose diagram is presented in **Fig. 4**. The maximum value of the bending moment occurs at the axle seat in the area of the joint with the wheel hub. Hence, the axle operates in

rotational bending conditions, which will be conducive to the generation of fatigue damage. That is why it is important to make an attempt to eliminate the focal points of fatigue.

It was assumed in the tests presented in this article that the load on the test model would be similar to that on wheel sets moving along a straight track without running onto the rail head. In such a situation, lateral forces will not occur, and only the forces originating from the vehicle weight will. The distribution of the bending moment following from such a load is presented in **Fig. 4**. As follows from the review of literature, lateral forces do not have significant influence on the initiation and development of fretting wear because of the sporadic occurrence of curves on the vehicle's route.

In view of the large dimensions of the wheel set, fretting wear tests on real object are more difficult because they require a special station. This is related to heavy expenditure and to a complicated joint disassembly procedure, which is why the tests were conducted on a simplified test model. It was demonstrated in works [L. 40, 41] that wear test results achieved on a model may be extrapolated to a real object.

## TEST METHODOLOGY

The purpose of the tests was to determine the actual condition of the top layer in the sleeve/shaft joint area after wear tests and the assessment of the influence of CrN+a-C:H:W coatings applied by means of the Physical Vapour Deposition on the development and intensity of fretting wear.

Tests of fretting wear in push fit joints were conducted on the model of a push fit joint of a rail vehicle wheel/wheel set axle, and the model consisted of a shaft and sleeve (**Fig. 2**). The model was assembled by pressing the sleeve onto the shaft with the tolerance of 0.02 mm. According to literature, surface pressures for the assumed tolerance value are most similar to surface pressures occurring in the actual wheel/axle joint.

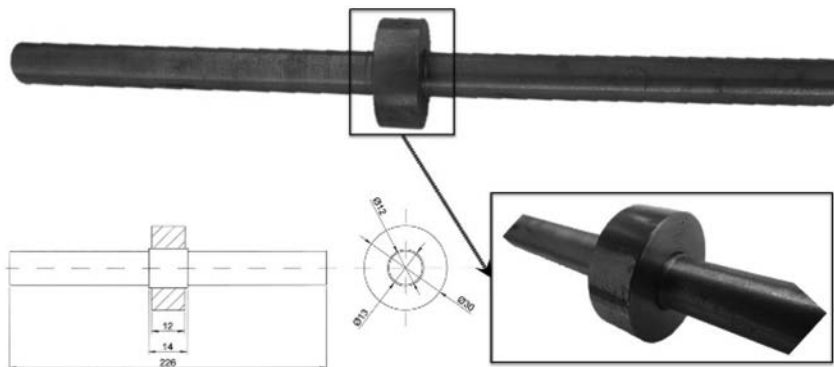


**Fig. 2. The general view of the test model; enlargement of the joint area and the dimensional scheme**

**Rys. 2. Widok ogólny modelu badawczego, powiększenie miejsca łączenia oraz schemat wymiarowy**



The maximum measured pressing force necessary for pressing the sleeve onto the uncoated shaft was 5 kN, and in the case of coated shafts, that force was 6 kN.

The presented test models were subjected to wear tests on a fatigue testing machine whose structure permits a periodically variable load with pure bending of a rotating sample.

The load on the test model was selected in a way enabling such a distribution of the bending moment which would cause sample deflection, as a result of which, during wear tests, oscillatory tangential displacement would occur between the mating elements, as was necessary for the initiation and development of fretting wear. In **Fig. 3**, a diagram of the model assembly in the fatigue testing machine and model loading is presented. The bending moment distribution under the presented load is similar to the bending moment distribution gained by a wheel set rolling along a straight track (**Fig. 4**).

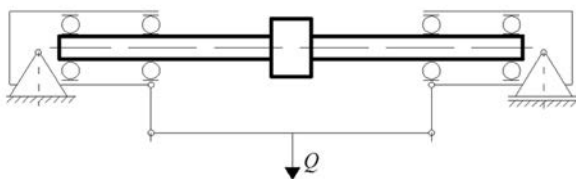


**Fig. 3. Test model assembly and load diagram**

Rys. 3. Schemat montażu i obciążenia modelu badawczego

The parameters of model tests at the fatigue testing machine were as follows:

- Model load:  $F = 550\text{ N}$ ,
- Bending moment:  $BM = 27.5\text{ Nm}$ ,
- Stress amplitude for shaft diameter 12 mm:  $118\text{ MPa}$ ,
- Stress amplitude for shaft diameter 13 mm:  $93\text{ MPa}$
- Number of cycles:  $n = 8 \times 10^6$ .

A FEM analysis in the ANSYS software was conducted for the assumed wear test parameters in order to check if appropriate shaft deflection needed for the generation of oscillatory tangential displacement would occur under the influence of those parameters as necessary for the initiation of fretting wear. The distribution of the displacement of model elements and surface stresses were analysed. The results of the analysis of the model elements' displacement are presented in **Fig. 5**.

The analysis demonstrated that the maximum displacement of the elements for the set point model testing parameters is 0.58 mm. That value should be sufficient for the generation of oscillatory tangential displacement. The results of the stress analysis are presented in **Fig. 6**.

Based on the analysis of surface stresses, it may be concluded that the assumed operation conditions will not lead to plastic deformation of the elements; the system will operate within the elastic deformation range. The maximum value of surface stresses is 356.65 MPa.

After the wear tests were completed, the test model was prepared for macro- and microscopic observations in conformity with the appropriate technology. Traditional

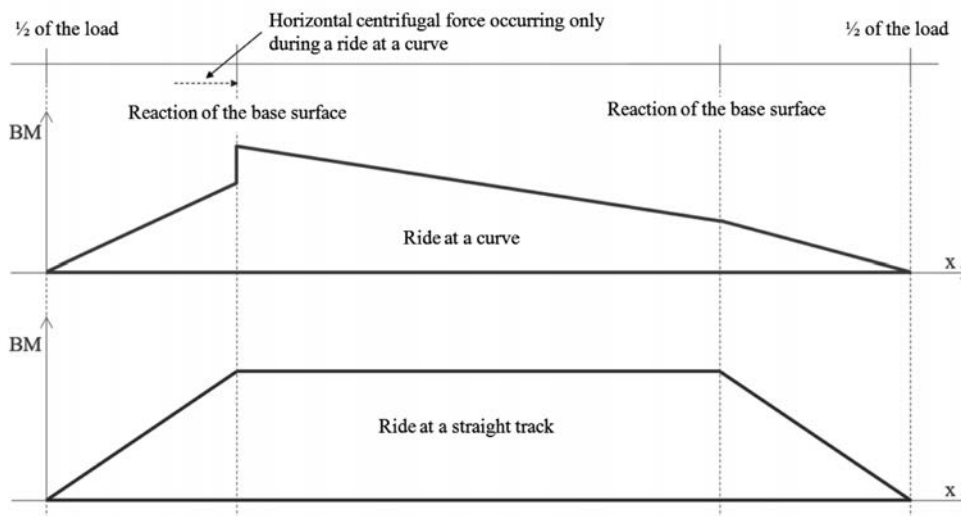


**Fig. 4. Bending moment distribution in the case of a ride at a curve and straight track**

Rys. 4. Rozkład momentu gñącego w przypadku jazdy pojazdu po łuku i torze prostym

forcing of the sleeve from the shaft could damage the fretting wear image and thus falsify the results. That is why the model was cut parallel to the shaft symmetry

axis and three samples were obtained in that way, which were then subjected to observations. First, macroscopic observations were conducted with a view to assessing the

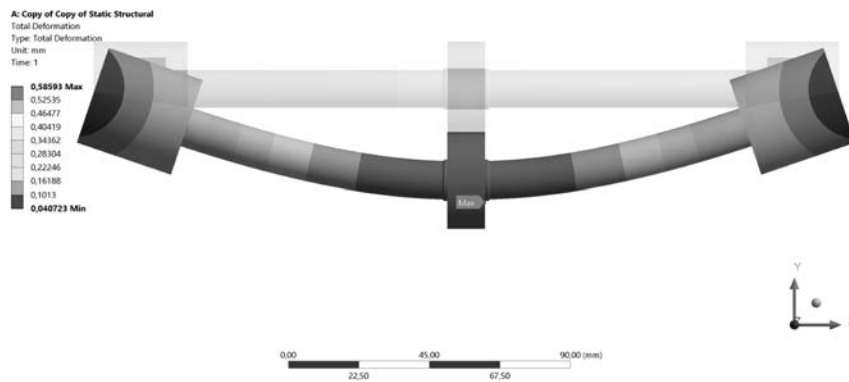


**Fig. 5. Result of the FEM analysis: distribution of the model's deflection lines**  
 Rys. 5. Wynik analizy MES: rozkład linii ugięcia modelu

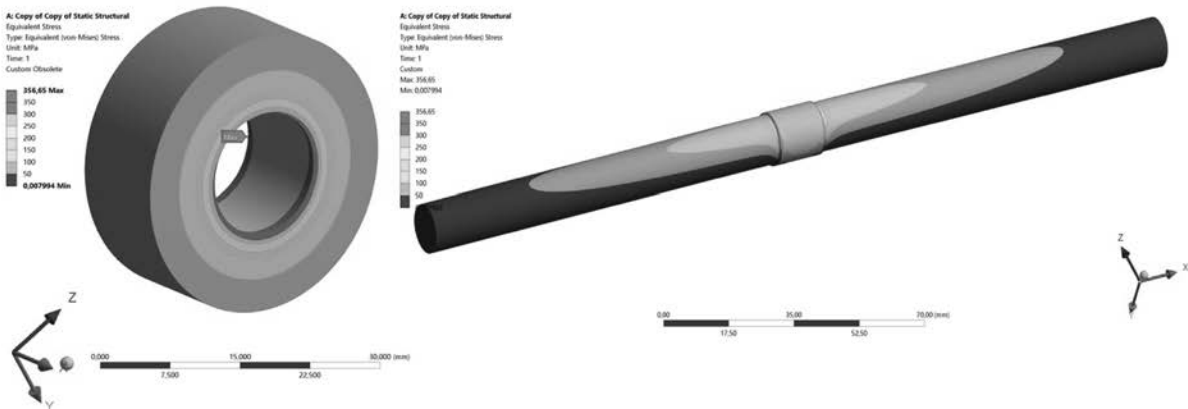


**Fig. 6. Result of the FEM analysis: stress distribution at the shaft and sleeve surface**  
 Rys. 6. Wynik analizy MES: rozkład naprężeń na powierzchni wału i tulei

condition of the top layer. Damage-affected areas were observed under a scanning microscope, which enabled the description of the kinds of damage comprised by fretting. An EDS microanalysis was also made, and so the chemical composition within the damage zone was identified at the surface and by volume.

### THE CHARACTERISTICS OF THE TOP LAYER OF TESTED SHAFTS

Shafts and sleeves made of C45 steel were used for the tests. The same material was the base surface for the coatings under analysis. Shafts were made in the turning process, without an additional finish treatment. The shaft top layer made in such a way had the roughness parameter  $R_a = 2.06 \mu\text{m}$ . The sleeve hub top layer was ground. Its roughness parameter  $R_a$  equals  $0.3 \mu\text{m}$ .

Shafts were covered with a CrN+a-C:H:W coating belonging to DLC coatings. This was applied to the shafts by means of the reactive spraying method in a physical

vapour deposition (PVD) process. The coating structure is presented in **Fig. 7**.

The coating consists of three layers and is colloquially called WC/C. The first layer is chromium nitride (CrN), whose task is to improve coating adhesion to the steel base surface. The next layer is tungsten carbide (WC), which protects the base surface against abrasion and is responsible for the transfer of high pressures. The third layer, called the external layer, directly mates with the sleeve. The coating thickness is  $4 \mu\text{m}$ .

The macroscopic image of the coated shaft top layer is presented in **Figure 8**. Observations with the use of a scanning microscope demonstrated that the coating under examination has a heterogeneous structure. Visible are conspicuous inclusions of tungsten carbide, which is a top layer component.

The coating under examination has microhardness HV0.05 equal to 1320. In the case of dry operation, the coefficient of friction is  $0.15 \mu\text{m}$ . The top layer's roughness parameter  $R_a$  equals  $1.68 \mu\text{m}$ .

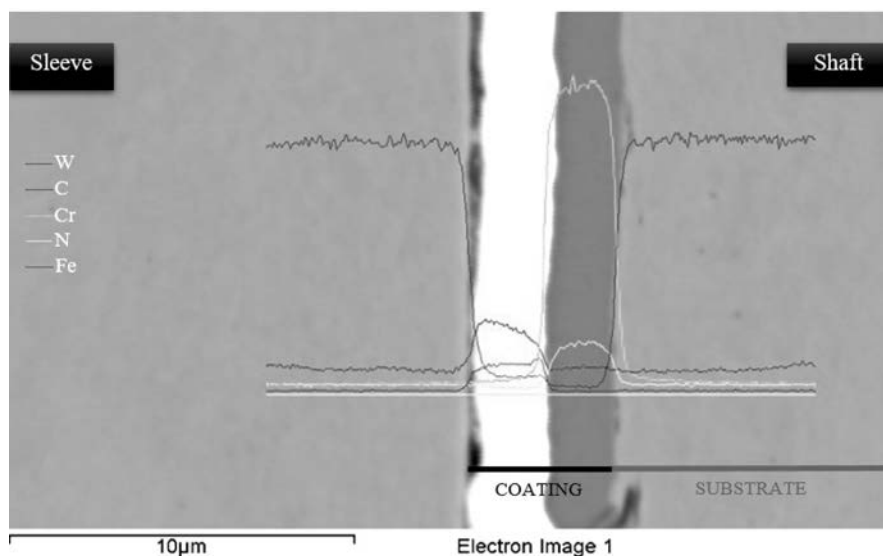


**Fig. 7. Cross-section of the test model with a coating structure**

Rys. 7. Przekrój poprzeczny modelu badawczego z zaznaczoną budową powłoki

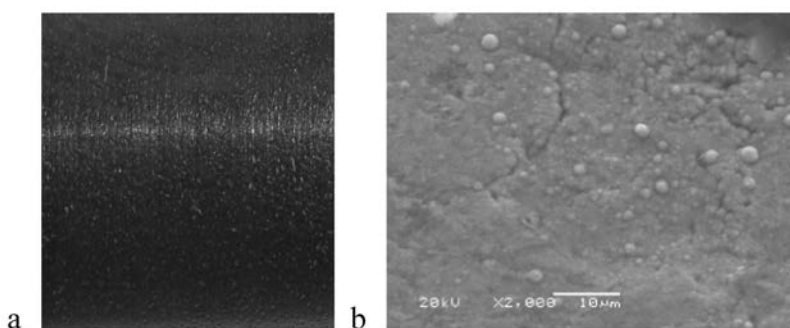


**Fig. 8. View of the top layer: a) the macroscopic image, b) the microscopic image**

Rys. 8. Widok warstwy wierzchniej: a) obraz makroskopowy, b) obraz mikroskopowy

## ANALYSIS OF TEST RESULTS

### *Uncoated shaft*

The results of the macroscopic observations of the uncoated shaft surfaces are presented in **Fig. 9**. Visible are traces of wear on either side of the axle seat. Traces of wear occur in the form of a ring occupying the entire circumference of the shaft axle seat and are of an intense nature. The width of the ring is approximately 2 mm on each side.

Such a large area affected by wear follows from a large contact area of the mating elements susceptible to the rise of adhesive bonds, particularly at joint edges.

Next, wear areas were observed under a scanning microscope to determine the kinds of wear comprised by fretting. A sample image is presented in **Fig. 10**. Visible is wear in the form of material build-up (the darker places). Additionally, wearing out and micro pits are found in



**Fig. 9. Macroscopic image of the uncoated shaft top layer**

Rys. 9. Obraz makroskopowy warstwy wierzchniej wału bez powłoki

places. Those kinds of damage are typical of adhesion, which will be leading in the case of forced-in joint. This also follows from the wear development mechanism discussed in detail by Guzowski S. in [L. 27]. The build-up arisen during joint assembly underwent plastic deformation during wear tests.

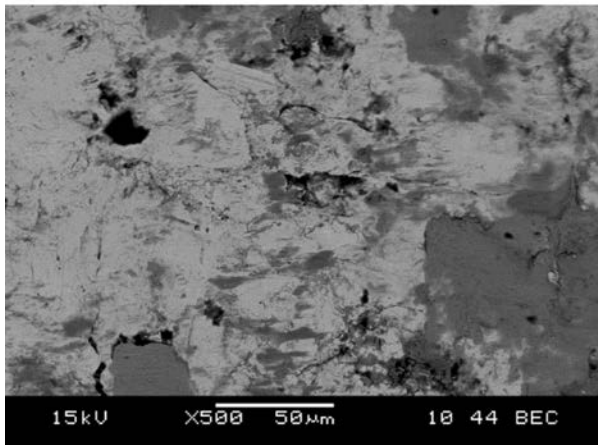


**Fig. 10. The SEM image at the place of fretting wear**  
Rys. 10. Obraz SEM w miejscu zużycia frettingowego

The EDS microanalysis of the chemical composition demonstrated the oxidation of the deformed build-up; hence, traces of wear observed on macroscopic photographs have a brown colour, which is characteristic of iron corrosion. Oxide formation is caused by sample deflection and the rise of a gap between the shaft and sleeve, which permits the contact of the damaged surface with oxygen.

#### Coated shaft

In the case of a coated shaft, traces of fretting wear are also observed. Their intensity is considerably smaller than on shafts without a coating. The dark colour of the coating blurs with brown traces of wear and prevents its identification with a naked eye; however, macroscopic observations at low magnification permit the distribution of wear to be exposed. Traces of wear occur at random on the axle seat circumference and are distinguished by a small area. The macroscopic image of the coated shaft top layer is presented in **Fig. 11**. Traces of fretting wear are marked with an arrow.

The lesser intensity of wear as observed at the shaft surface confirms the partial elimination of adhesion, which is one of the causes of fretting wear development. The greater roughness of the shaft surface reduces the risk of adhesive bond formation during joint assembly.

Observations of the places of fretting wear with the use of a scanning microscope disclosed a similar character of wear as in the case of uncoated shafts. Material build-up undergoing plastic deformation is also observed. The EDS analysis of the chemical composition in the wear zone (**Fig. 12**) demonstrated that such build-up

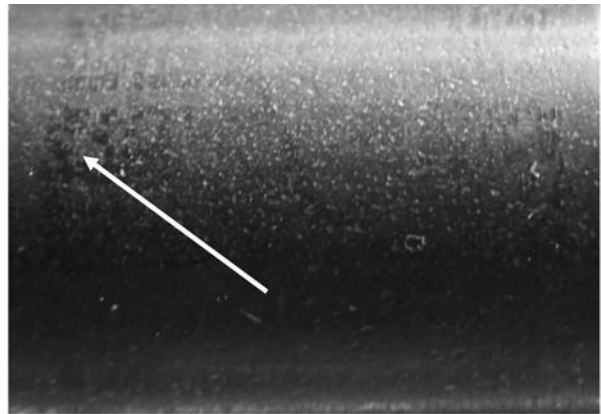


**Fig. 11. Macroscopic image of the coated shaft top layer**  
Rys. 11. Obraz makroskopowy warstwy wierzchniej wału z powłoką

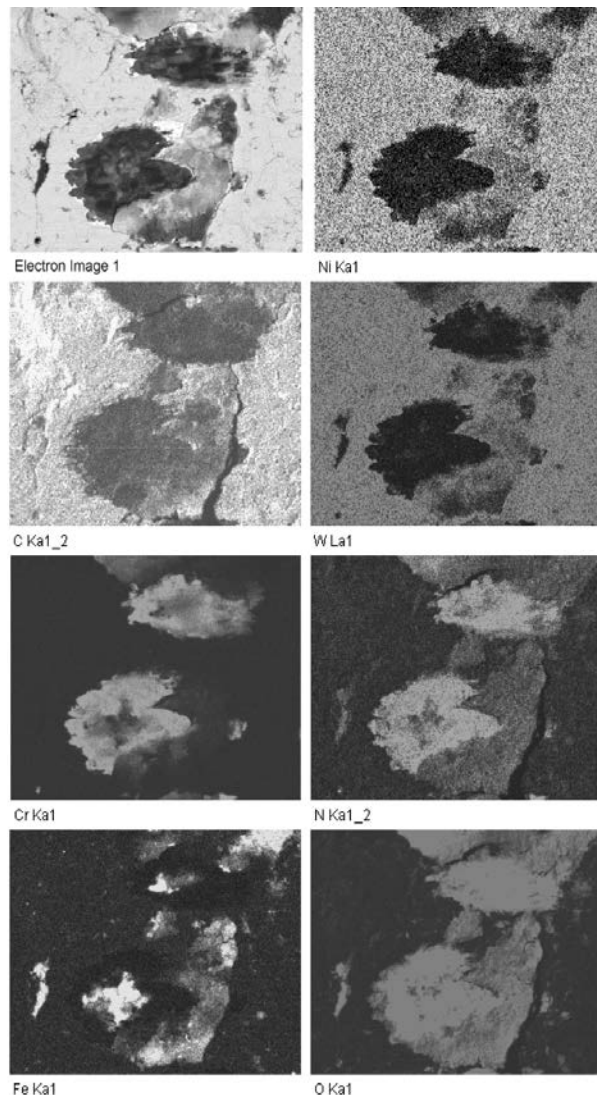


**Fig. 12. Chemical element distribution maps for the fretting wear zone**  
Rys. 12. Mapy rozkładu pierwiastków chemicznych w strefie zużycia frettingowego



originates from the shearing of micro-irregularities of the sleeve top layer, a fact confirmed by the iron distribution map. That build-up became oxidised during wear tests, which is also confirmed by the oxygen distribution map. The coating became damaged in places. Hence, in the EDS analysis, visible are chromium and nitrogen, which are the elements that constitute the intermediate layer whose task is to improve the adhesion properties of the proper coating with the base surface. The complete damage of the coating occurred in several places, and the base surface was uncovered, which is also visible in the analysis. Nickel observed in the area under analysis is a result of the technological preparation of the coating for testing.

## CONCLUSIONS

The purpose of the tests was to determine the actual condition of the top layer in the sleeve/shaft joint area after wear tests and the assessment of the influence of the coatings under analysis on the development and intensity of fretting wear.

Macroscopic observations of the top layer of the shafts under analysis demonstrated the presence of the traces of fretting wear both in the case of shafts with and without a coating.

The tests of the test model without a coating confirmed that the assumptions concerning the assumed model and test methodology were correct. Samples did not undergo plastic deformation, and the nature of the observed image of wear corresponds to the examples given in literature. Wear is located on either side of the axle seat, approximately 2 mm from the edge, and takes the form of a ring with a specific width comprising the entire axle seat circumference.

Macroscopic observations of the models with coated shafts showed a clear influence of the tribological properties of the coating on fretting wear development. Wear intensity is significantly smaller, traces of wear are visible at the axle seat circumference in places, and the areas affected by wear are small.

Macroscopic observations of the surface of all the shafts demonstrated the common typical features of wear, such as the brown colour at the place of the damage of the surfaces being examined or the location of wear on either side of the axle seat, close to the joint edges.

Microscopic observations of the areas affected by wear show the similar character of damage on all of the analysed samples. First of all, material build-up was observed that arose during joint assembly and stemmed from the shearing of micro-irregularities of the top layer of the mating elements. In the case of test models with a coating, that build-up originates from the shearing of micro-irregularities of the sleeve top layer, which was confirmed by the x-ray microanalysis by means of the EDS method. Microanalysis also demonstrated that the earlier plastically deformed build-up becomes oxidised during wear tests. In addition to material build-up, microcracks, local coating chipping, and micro pits were observed.

The coating used not only mitigates fretting wear development but also improves the life of the elements. Uncoated shaft cracking took place after  $8 \times 10^6$  cycles, and the coated shaft cracking took place after  $20 \times 10^6$  cycles.

Based on the tests, it may be concluded that the analysed coatings may be used for the protection of the elements connected by pressing and operating in rotational bending conditions from fretting wear development.

## REFERENCES

1. Madej M., Ozimina D.: The tribological properties of diamond-like carbon coatings under ionic liquids lubrication. *Tribology* 4 (2014), pp. 73–84.
2. Aisenberg S., Chabot R.: Ion-beam deposition of thin film soft diamond like carbon. *Journal Applied Physics*. 42 (1971), pp. 2953–2956.
3. Igartua A., Berriozabal E., Nevshupa R., Roman E., Pagano F., Pleth Nelson L., Louring S., Muntada L.: Screening of diamond-like carbon coatings in search of a prospective solid lubricant suitable for both atmosphere and high vacuum applications. *Tribology International* 114 (2017), pp. 192–200.
4. Mabuchi Y., Higuchi T., Yoshimura D., Murashima M., Kousaka H., Umehara N.: Influence of carbon black in engine oil on wear of H-free diamond-like carbon coatings. *Tribology International* 73 (2014), pp. 138–147.
5. Zhang Y., Polychronopoulou K., Humood M., Polycarpou A.A.: High temperature nanotribology of ultra-thin hydrogenated amorphous carbon coatings. *Carbon* 123 (2017), pp. 112–121.
6. Martini C., Ceschini L., Casadei B., Boromei I., Guion J.B.: Dry sliding behaviour of hydrogenated amorphous carbon (a-C:H) coatings on Ti-6Al-4V. *Wear* 271 (2011), pp. 2025–2036.
7. Makowski S., Schaller F., Weihnacht V., Englberger G., Becker M.: Tribochemical induced wear and ultra-low friction of superhard ta-C coatings. *Wear* 392–393 (2017), pp. 139–151.

8. Wang Q., Zhou F., Wang C., Yuen Muk-Fung, Wang M., Qian T., Matsumoto M., Yan J.: Comparison of tribological and electrochemical properties of TiN, CrN, TiAlN and a-C:H coatings in simulated body fluid. *Materials Chemistry and Physics* 158 (2015), pp. 74–81.
9. Gies A., Chudoba T., Schwarzer N., Becker J.: Influence of the coating structure of a-C:H:W coatings on their wear-performance: A theoretical approach and its practical confirmation. *Surface & Coatings Technology* 237 (2013), pp. 299–304.
10. Dowling D.P., Kola P.V., Donnelly K., Kelly T.C., Brumitt K., Lloyd L., Eloy R., Therin M., Weill N.: Evaluation of diamond-like carbon-coated orthopaedic implants. *Diamond and Related Materials* Volume 6, Issues 2–4 (1997), pp. 390–393.
11. Hauert R.: A review of modified DLC coatings for biological applications. *Diamond and Related Materials* Volume 12, Issues 3–7 (2003), pp. 583–589.
12. Hing H.A., Choudhury D., Nine M.J., Osman N.A.A.: Effects of surface coating on reducing friction and wear of orthopaedic implants. *Sci. Technol. Adv. Mater.* 15 (2014), pp. 1–21.
13. Bill R. C. Fretting wear and fretting fatigue – How are they related? *Journal of Lubrication Technology* 1983; 105 issue 2, pp. 230–238.
14. Guo X., Lai P., Tang L., Wang J., Zhang L.: Effects of sliding amplitude and normal load on the fretting wear behavior of alloy 690 tube exposed to high temperature water. *Tribology International* 116 (2017), pp. 155–163.
15. Majzooobi G.H., Abbasi F.: On the effect of shot-peening on fretting fatigue of Al7075-T6 under cyclic normal contact loading. *Surface and Coatings Technology* 328 (2017), pp. 292–303.
16. Li X., Yang J., Li M., Zuo Z.: An investigation on fretting fatigue mechanism under complex cyclic loading conditions. *International Journal of Fatigue* 88 (2016), pp. 227–235.
17. Lu W., Zhang P., Liu X., Zhai W., Zhou M., Luo J., Zeng W., Jiang X.: Influence of surface topography on torsional fretting wear under flat-on-flat contact. *Tribology International* 109 (2017), pp. 367–372.
18. Budinski K.G.: Effect of hardness differential on metal-to-metal fretting damage. *Wear* volume 301 issues 1–2 (2013), pp. 501–507.
19. Lemm J.D., Warmuth A.R., Pearson S.R., Shipway P.H.: The influence of surface hardness on the fretting wear of steel pairs – Its role in debris retention in the contact. *Tribology International* 81 (2015), pp. 258–266.
20. Kesavan D., Done V., Sridhar M.R., Billing R., Nelias D.: High temperature fretting wear prediction of exhaust valve material. *Tribology International* 100 (2016), pp. 280–286.
21. Cai Z., Zhu M., Shen H., Zhou Z., Jin X.: Torsional fretting wear behaviour of 7075 aluminium alloy in various relative humidity environments. *Wear* volume 267, issues 1–4 (2009), pp. 330–339.
22. Zhang P., Liu X., Lu W., Zhai W., Zhou M., Wang J.: Fretting wear behavior of CuNiAl against 42CrMo4 under different lubrication conditions. *Tribology International* 117 (2018), pp. 59–67.
23. English R., Ashkanfar A., Rothwell G.: A computational approach to fretting wear prediction at the head-stem taper junction of total hip replacements. *Wear* 338–339 (2015), pp. 210–220.
24. Zasińska K., Seramak T., Łubiński J.I.: Comparison of the abrasion resistance of the selected biomaterials for friction components in orthopedic endoprostheses. *Tribology* 6 (2015), pp. 187–198.
25. Gil F. J., Canedo R., Padrós A., Bañeres M.V., Arano J.M.: Fretting corrosion behaviour of ball-and-socket joint on dental implants with different prosthodontic alloys. *Bio-Medical Materials and Engineering* 13 (2003), pp. 27–34.
26. Kralya V.O., Molyar O.H., Trofimov V.A., Khimko A.M.: Defects of steel units of the high-lift devices of aircraft wings caused by fretting corrosion. *Materials Science* 46 (2010), pp. 108–114.
27. Lee B. -W., Suh J., Lee H., Kim T.-G.: Investigations on fretting fatigue in aircraft engine compressor blade. *Engineering Failure Analysis* 48 issue 7 (2011), pp. 1900–1908.
28. Sujata M., Madan M., Raghavendra K., Bhaumik S.K.: Fretting Fatigue in Aircraft Components Made of Ti–Al–V Alloys. *Procedia Engineering* 55 (2013), pp. 481–486.
29. Giacco del M., Weisenburger A., Zimmermann P.S.F., Lang F., Muller J.G.: Experimental equipment for fretting corrosion simulation in heavy liquid metals for nuclear applications. *Wear* 280–281 (2015), pp. 46–53.
30. Blau P.J.: A multi-stage wear model for grid-to-rod fretting of nuclear fuel rods. *Wear* 313 issues 1–2 (2014), pp. 89–96.
31. Fei Xue, Zhao-Xi Wang, Wen-Sheng Zhao, Xiao-Liang Zhang Bao-Ping Qu LiuWei: Fretting fatigue crack analysis of the turbine blade from nuclear power plant. *Engineering Failure Analysis* 44 (2014), pp. 299–305.
32. Wang D., Zhang D., Se S.: Effect of terminal mass on fretting and fatigue parameters of a hoisting rope during a lifting cycle in coal mine. *Engineering Failure Analysis* 36 (2014), pp. 407–422.
33. Wang D., Zhang D., Zhao W., Ge S.: Quantitative analyses of fretting fatigue damages of mine rope wires in different corrosive media. *Materials Science and Engineering: A* 596 (2014), pp. 80–88.

34. Collini L., Degasperi F.: MRT detection of fretting fatigue cracks in a cableway locked coil rope. *Case Studies in Nondestructive Testing and Evaluation* 2, (2014), pp. 64–70.
35. Panda B., Balasubramaniam R., Mahapatra S., Dwivedi G.: Fretting and fretting corrosion behavior of novel micro alloyed rail steels. *Wear* 267 issues 9–10 (2009), pp. 1702–1708.
36. Zheng J.F., Luo J., Mo J.L., Peng J.F., Jin X.S., Zhu M.H.: Fretting wear behaviors of a railway axle steel. *Tribology International* 43 issues 5–6, (2010), pp. 906–911.
37. Guzowski S., Michnej M.: Influence of technological methods increasing surface layer durability on axles fretting wear in railway wheel sets. *Eksploatacja i Niezawodność – Maintenance and Reliability* 18 issue 1 (2016), pp. 1–9.
38. Zhang Y., Lu L., Gong Y., Zhang J., Zeng D.: Fretting wear–induced evolution of surface damage in press–fitted shaft. *Wear* 384–385 (2017), pp. 131–141.
39. Guzowski S.: *Analysis of fretting wear in clamped joints on example of rail vehicle wheelset axles*. Krakow: Cracow University of Technology Press, 2003.
40. Guzowski S.: Simulation of axle set fretting fatigue in model testing. *The Proceedings of the 10<sup>th</sup> Congress on Material Testing* vol. 2, Budapest 1991, pp. 478–483.
41. Kowalski S.: Application of dimensional analysis in the fretting wear studies. *Journal of the Balkan Tribological Association* 2016; 22(4), pp. 3076–3088.